Fatty Acid Kinetics in Aerobic Myocardium: Characteristics of Tracer Carbon Entry and Washout and Influence of Metabolic Demand

Stephen H. Nellis, A. James Liedtke, and Britta Renstrom

Cardiology Section, University of Wisconsin Hospital and Clinics, Madison, Wisconsin

These studies evaluated the kinetics of tracer uptake and washout after step-function labeling with ^{14}C-palmitate. Washout and uptake function curve analysis for total radioactivity (TR) was derived according to the expressions:

$$TR = Fx \int_0^\infty C(t) \times dt$$

and

$$TR = Fx \int_0^\infty (C_{ss} - C(t)) \times dt,$$

respectively, with $V_C = \frac{TR}{C_a}$,

where F = coronary flow; C_{ss} = steady-state concentration; $C(t)$ = concentration with respect to time; C_a = arterial concentration; and V_c = distribution volumes within the fatty acid pathway. The only radioactive metabolites in venous effluent were fatty acids and $^{14}CO_2$. The estimated V_c of fatty acids was small (1.2–1.7 ml/g dry wt or 0.4–0.5 μmol/g dry wt) and compatible with labeled substrate trapped in the blood volume. The V_c of $^{14}CO_2$ was much larger (11.4–15.8 ml/g dry wt or 3.6–4.2 μmol/g dry wt) and correlated with counts contained in the aqueous soluble and fatty acid fractions in tissue. The counts in tissue were distributed between the aqueous soluble fraction (40%), which was rapidly depleted during washout, and a lipid fraction (60%) (triacylglycerols and phospholipids), which was resistant to washout. Distributions in tissue radioactivity between the aqueous soluble and lipid fractions support the notion of a dual pathway in fatty acid oxidation, one arm of which passes through the resident pool of triacylglycerols, which has a long time constant. The presence of this pool may impart an error in estimating fatty acid oxidation by external labeling techniques.

J Nucl Med 1992; 33:1864–1874

The application of "trace"-labeled biological compounds to measure key processes of intermediate metabolism in heart muscle has traditionally relied on steady-state, equilibrium-labeled, infusion methods. With this approach, tagged substrates representing fatty acids, carbohydrates, amino acids or ketone bodies, and labeled with radioactive atoms, are supplied to the myocardium at a constant concentration for a sufficient length of time to allow the atoms to reach a constant level within the metabolic pathway of interest. As an example, [U-^{14}C] palmitate is frequently infused into the coronary circulation for minutes to hours (*1–3*), and the veno-arterial difference of $^{14}CO_2$ measured to estimate the rate of fatty acid oxidation at various perfusion conditions. There is evidence in some circumstances, however, that the oxidation of palmitate estimated by this method, even following relatively long (30 min) periods of substrate equilibrium-labeling, does not reflect the total oxidation of free fatty acids (*4*). This may result from the interaction of carbon pools within the cardiomyocyte which are exchangeable with the trace carbon but have not yet reached equilibrium. Such would be the case particularly for the large storage pool represented by neutral lipids. Specifically, Hansen et al. (*4*) have suggested that the large, endogenous stores of fatty acids contained in complex tissue lipids do not easily or quickly equilibrate with extracted fatty acids from the perfusate even when the $^{14}CO_2$ from exogenous fatty acids has reached an apparent steady state production level in coronary venous effluent.

With these issues yet to be resolved, the purpose of the present study was to examine the uptake and washout of tracer carbon from ^{14}C-palmitate after a step-function increase or decrease of isotope administered to the coronary perfusate at aerobic flows. A specific interest was to quantitate the influence of triacylglycerols in contributing labeled fatty acids to the fatty acid utilization pathway following exogenous labeling. The goals were to apply a technique which was sensitive to events within the entire metabolic pathway and to mathematically analyze the data with few assumptions. Efflux of metabolites and $^{14}CO_2$ from the heart was surveyed within the time encompassed by the two or more distinct time constants manifest in ^{14}C-palmitate metabolism (*6,7*). Uptake and washout curve analyses were selected to permit a testing of the hypothesis of whether or not equilibrium of ^{14}C-labeled

Received December 10, 1991; revision accepted May 20, 1992

For reprints contact: Stephen H. Nellis, PhD, Cardiology Section, University of Wisconsin Hospital and Clinics, 600 Highland Ave., H6/339 CSC, Madison, WI 53792.

long-chain fatty acid substrate occurred within predicted times of coronary perfusion. Experiments were conducted in extracorporeally perfused aerobic pig hearts. A companion paper to this describing similar events in coronary reperfusion following regional myocardial ischemia has recently been published (*8*).

METHODS

Surgical Preparation

Adolescent swine (average weight 49 ± 0.8 kg) fasted overnight were studied after anesthesia with pentobarbital (35 mg/kg i.v.) and the establishment of positive pressure ventilation with oxygen-supplemented room air. Additional drug was given as needed to ensure adequate anesthesia throughout the experiments. Frequent determinations of arterial blood gases were done to ensure adequate ventilation and acid-base balance. Studies were performed in an open-chest, intact, working heart preparation which has been extensively described previously (*1,8–13*). After a bilateral thoracotomy and treatment with heparin (10,000 U/hr i.v.), a surgical arterioarterial shunt was constructed extracorporeally connecting a femoral artery with the coronary arteries. The left main coronary artery was cannulated with a Gregg cannula inserted retrogradely from the left subclavian artery, while the right coronary artery was perfused by a cannula positioned near its origin. The left anterior descending (LAD) artery was perfused separately with a cannula placed near its bifurcation from the circumflex artery. The circumflex artery was then perfused through the Gregg cannula. Flow in all three circuits was supported by three separate, extracorporeal perfusion pumps. Flow in the right and main left coronary arteries was set by adjusting their respective perfusion pressures to 10–20 mmHg above average aortic pressure. Cumulatively, these flows equaled 11.2 ± 0.5 ml min^{-1} g dry wt^{-1}. Flow in the LAD bed was fixed at 6.9 ± 0.3 ml min^{-1} g dry wt^{-1} by keeping pressure in the LAD perfusion circuit, corrected for cannula resistance, at that of average aortic pressure. Also contained in the LAD perfusion circuit were three access ports. One port allowed infusion of Indocyanine green directly into the circuit through a 50 ml mixing chamber. Another port was for infusion of ^{14}C-palmitate and was connected to a special section within the perfusion circuit (volume 8 ml) consisting of alternate segments of small (¼ in. i.d.) and large (½ in. i.d.) tubing which were used for mixing the tracer with the whole blood perfusate. A venous cannula was inserted into the great cardiac vein anteriorly, which together with the third arterial port, was used to sample for gases and metabolites across the anterior perfusion bed. A 7F high-fidelity micromanometer-tipped catheter was placed in the left ventricle to monitor pressures.

Indocyanine green dye was infused over 5 min (1 ml/min) of each 10-min sampling interval to estimate venous cross-contamination and dilution in the LAD venous circulation (*12,13*). Samples of arterial and venous blood from the LAD circuit were collected at 0, 10, 20, 30 and 40 min in uptake studies and at 0, 20, 40, 50, 60, 70 and 80 min in washout studies and the ratio of venous-to-arterial concentrations of green dye was used to derive a correction factor for radioactive counts obtained in the venous samples. There was no appreciable (<9% after 80 min) recirculation of dye returning from the periphery to contaminate the measurements.

Protocol

The study was divided into two parts. For the main protocol in 13 animals, ^{14}C-palmitate was infused for 43.2 ± 1.1 min, while blood samples were obtained as described below. At the end of this time period, the animals were killed and tissue samples obtained. For the second protocol in seven animals, the radioactive palmitate was infused for 40 min after which the infusion was terminated. Samples of perfusate blood and venous effluent were obtained for another 40 min thereafter to follow the washout of the radioactivity from the heart (in one animal this period of washout was extended to 60 min). Tissue samples were obtained at the completion of these studies as well. In both protocols, heart rate was allowed to vary while regional coronary perfusion and ventricular pressures were controlled.

Metabolic data were collected as follows: venous $^{14}CO_2$ at 2-min intervals; arterial $^{14}CO_2$ at 10-min intervals; venous plasma at 0.5-min intervals for 3 min, then at 2-min intervals thereafter; LAD and femoral arterial plasma at 10-min intervals; and venous and arterial blood for extraction with perchloric acid at 10-min intervals. Blood gases were obtained at 10-min intervals. Regional myocardial oxygen consumption was modified from a previously described expression using blood gas data and LAD flow (*14*).

At the conclusion of each study, to avoid any washout of radioactivity, infusion of labeled palmitate was continued until tissue biopsies from the LAD and circumflex (LCF) beds were taken. The interval between acquiring the last blood samples and obtaining the biopsies was <4 min. The tissue samples were frozen with Wollenberger clamps and stored at −70°C until analyzed. India ink was injected into the LAD cannula and the perfusion beds dissected free and weighed.

Chemical Procedures

Blood samples were obtained from the LAD artery and vein at the time intervals described above. Three 1.0 ml samples of this blood were used for $^{14}CO_2$ determination by injecting 1.0 ml into a sealed Erlenmeyer flask containing 0.5 ml concentrated sulfuric acid and a centerwell with methylbenzethonium hydroxide as a CO_2 absorber. After 45 min, the centerwell was transferred to a liquid scintillation vial containing a compatible cocktail and the content measured for radiocarbon. The remainder of the blood collected above was centrifuged at 1,500 × g at 4°C for 10 min to yield plasma. Blood from the femoral artery was likewise centrifuged for plasma determination only. Plasma aliquots were added to 0.1 ml of 2 N hydrochloric acid to drive off any dissolved CO_2 and after 45 min neutralized with 0.1 ml of 2 N sodium hydroxide before measuring total radiocarbon. This was used in recovery experiments to be described below. The remainder of the plasma was frozen for later analysis of free-fatty acids.

One milliliter of blood from the LAD artery and vein was also obtained in a syringe already containing 1.0 ml of 0.6 *M* perchloric acid. The contents were thoroughly mixed, allowed to stand on ice for at least 5 min and centrifuged at 1,500 × g at 4°C for 10 min to remove precipitated protein. The resulting supernatant was stored frozen for later analysis of organic acid soluble compounds by high-performance liquid chromatography (HPLC).

The quantification of these acid soluble products was conducted using a modified method of Pokits et al. (*15*). The protein-free supernatant derived above for HPLC analysis was injected directly into a Bio Rad Aminex HPX-87H HPLC column (300 × 7.8 mm) using 0.01 N sulfuric acid in an exponential gradient

up to 10% acetonitrile at a flow rate of 0.6 ml/min. Absorbance was recorded at 193 nm (necessary to detect glucose) and peak areas were compared to corresponding standards. The column effluent was collected by a Gilson Model 203 Micro Fraction Collector directly into liquid scintillation vials. Using peak-detection algorithms, selective collection of products was obtained and radiocarbon levels determined. Recovery studies of this HPLC plasma extract were also done to identify any other unknown products. The extract was first counted, then applied to HPLC and the above fractions collected and counted.

Free fatty acids were extracted from blood plasma and the total free fatty acid content determined using the ^{63}Ni assay according to the methods of Ho (*16*). For an initial separation of lipids into general classes, plasma samples were extracted with chloroform and methanol after the method of Bligh and Dyer (*17*). This extraction also left an aqueous fraction which was counted for radiocarbons. Separation of neutral lipids, free fatty acids and polar lipids was obtained following the method of Hamilton and Comai (*18*) using prepacked silica Sep-Pak columns. A residual was left in the vial which was counted. The isolated fractions were also counted for radiocarbon. In separate experiments a blood sample was taken before any radioactivity was introduced into the animal. Carbon-14-palmitate in 3% BSA was added and the sample processed as described. The counts from these samples were used as a standard to which the main samples were compared. Tissue was likewise extracted with chloroform and methanol and the lipids separated by silica Sep-Pak columns as described above for plasma.

The chloroform extract from above was also dried, after which 3% BSA was added and the mixture stirred for 3 hr. Triacylglycerols were then measured using a Triglyceride [UV] kit from Sigma. The triacylglycerols were also estimated as free fatty acids after hydrolysis with KOH using the Wako enzymatic kit for free fatty acid determination. Both methods gave the same results.

Total tissue radioactivity was obtained by digesting tissue in a tissue solubilizer and the resulting solution counted for radiocarbon. The scheme for fractionating the blood and tissue fractions is shown in Figure 1. The radioactivity in the tissue was expressed in two units. First, arterial specific activity in dpm/mol free fatty acid was used to express the tissue concentration of counts in terms of the equivalent moles of free fatty acid/g dry wt of the tissue metabolite. Second, the radioactivity (in dpm/g dry wt) in the tissue fraction was normalized by the radioactivity in the arterial blood (in dpm/ml). The resulting units of this second derivation were ml/g dry wt which were comparable to the radioactive uptake calculations from the venous time-concentration curves (see Results section). Blood radioactivity was also expressed by the same two units.

Statistical analysis of the kinetic data was performed using paired and nonpaired Student's t-tests and correlations were estimated with multiple linear regressions. Probability values for statistical significance are listed as 5% or less by two-tailed comparisons.

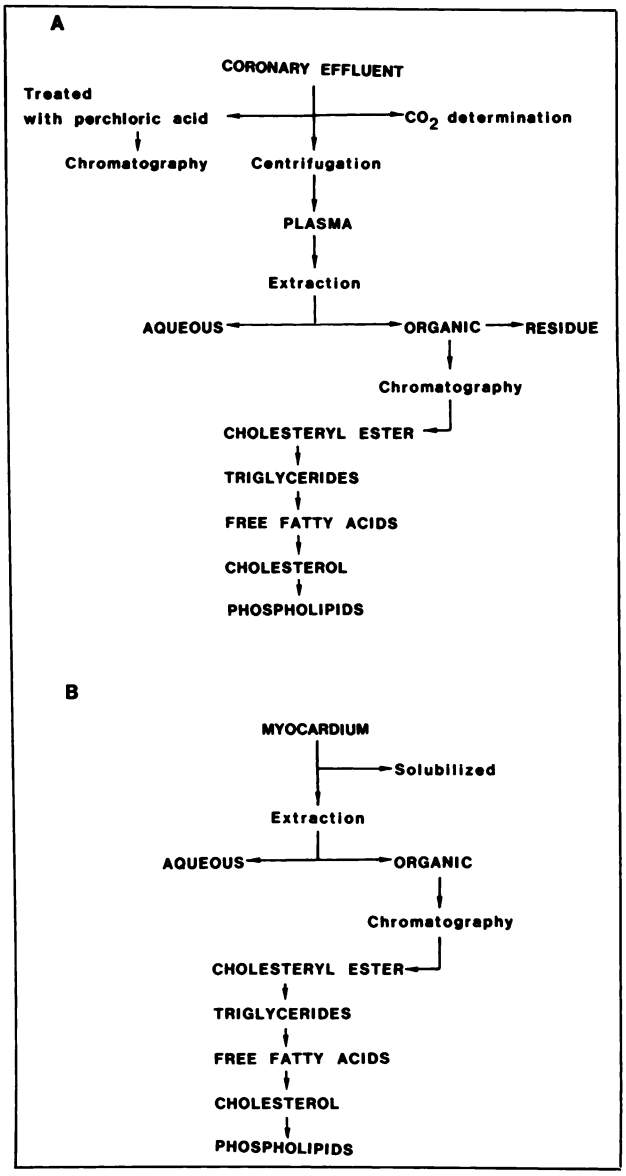

FIGURE 1. Flow chart of strategies to identify distributions of radioactivity in possible metabolites derived from fatty acid utilization which are contained either in coronary effluent (A) or myocardium (B).

RESULTS

Theoretical Considerations

The major goal of this study was to develop uptake and washout curves using step-function increases or decreases of ^{14}C-palmitate in order to estimate distribution volumes of fatty acid metabolites in aerobically perfused myocardium. A model of the infusion technique employed and the consequent uptake curves used in this approach are shown in Figure 2A. The difference between the rate by which radioactivity leaves the heart through the venous effluent and that which enters from the arterial perfusate represents the instantaneous radioactive uptake by the heart. The integration of this difference represents the total pool size of material taken up by the heart. Two problems must be dealt with in this approach. The first is anatomical and involves recovery of label. That is to say, blood sampled from the anterior vein does not all originate from the LAD coronary artery and may be slightly contaminated (≤10%) with blood from other vessels (*19,20*). Therefore, venous radioactivity is not equal to arterial radioactivity even without myocardial uptake of labeled

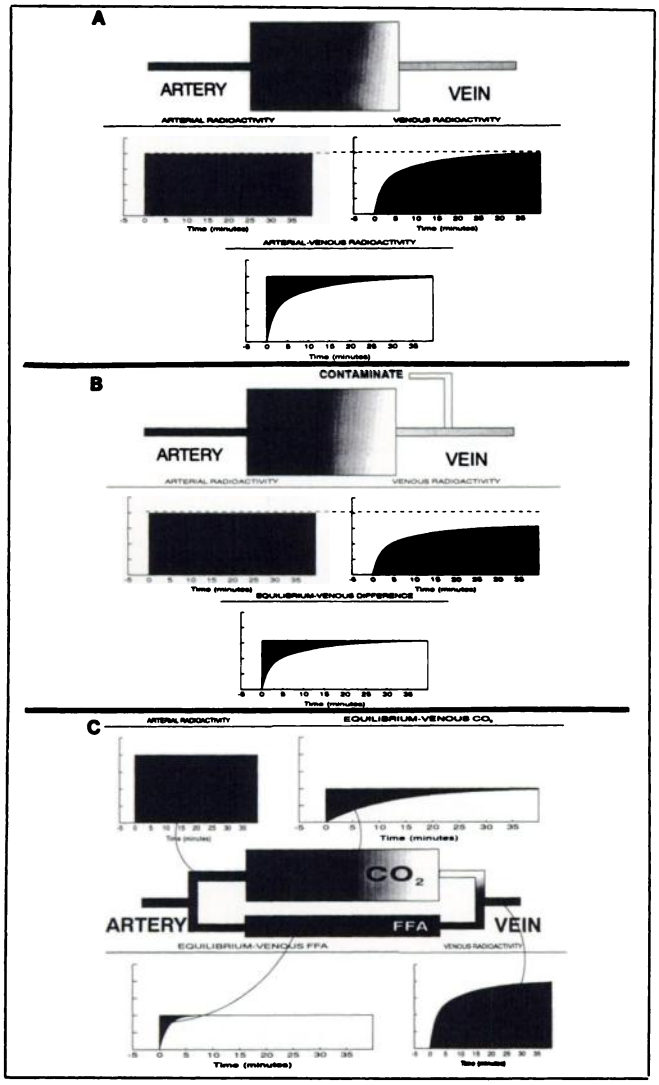

FIGURE 2. The integration of the venous efflux minus the arterial influx curve (A) uses the principle of the conservation of mass to calculate the radioactive uptake of the heart (shaded area, bottom curve). At steady-state in the ideal system, the venous efflux is equal to the arterial influx (dashed line). (B) With contamination of the venous blood, however, the venous efflux never attains the value of the arterial influx. Accurate determination of the instantaneous venous-arterial differences cannot be determined. The integration, however, can be approximated by evaluating the difference between the equilibration value and the instantaneous venous content as shown in the bottom curve. (C) This concept can be extended to analyzing the radioactivity of individual compounds (CO_2 and FFA) so that the total radioactive uptake can be divided between different terminal metabolites of interrelated pathways.

material. In our studies, venous dilution is measured with indocyanine green dye and corrections applied to venous samples to compensate for this contamination. However, even after such corrections there are small (<2%) errors. These errors are inconsequential for most applications but in these studies would accumulate when integrating over relatively long perfusion times. Nevertheless, venous radioactivity becomes equal to arterial radioactivity at equilibrium. Thus, rather than measuring venous-arterial differences of radioactivity in perfusate, using the principles of equilibrium labeling, it is possible to integrate counts in venous effluent only and estimate myocardial uptake of radioactive material as the difference between venous and steady-state levels of radioactivity (Fig. 2B).

The second problem deals with specificity and the limitations inherent in quantitating venous-arterial differences of total radioactivity. Radioactivity potentially exits the heart in more than one compound. Each compound represents a different terminus of interactive metabolic pathways. In these studies we surveyed several such compounds (Fig. 1A). By examining the radioactive uptakes of these compounds (as an example, see analyses for fatty acids and CO_2 in Fig. 2C), the total radioactive pools can be separated into constitutive pools representing the end-metabolites of different metabolic pathways. For these studies, we examined carbon pools displaced by radioactive fatty acids as the radioactive carbons traveled through the fatty acid utilization pathway and were either oxidized to $^{14}CO_2$ or exited as other specific metabolites in the coronary venous effluent. Total radioactivity (TR) is expressed mathematically as:

$$TR = F_c \times \int_0^{\infty} \left(C_{ss} - C(t)\right) \times dt \qquad \text{Eq. 1}$$

and

$$V_c = TR \div C_a, \qquad \text{Eq. 2}$$

where V_c is the distribution volume of the carbon pool size, F_c is the coronary flow, C_{ss} is the steady-state concentration of radioactive end-metabolites in venous blood, C(t) is the concentration of radioactive metabolites in venous effluent as a function of time and C_a is the coronary arterial concentration of radioactivity.

The integration for TR describes uptake in disintegrations per minute (dpm). The total radioactive uptake was normalized by the tissue weight of the LAD-perfused bed so that the final units were dpm/g dry wt. While this estimate of radioactive uptake can provide useful information, it is often an equivocal expression since the units depend not only on the physiology of the heart but also on the concentration of the trace-labeled and cold metabolite in arterial blood. This dependence can be eliminated or minimized by alternate normalizations. Two different descriptive approaches were used. The simplest approach was to normalize TR by the arterial radioactivity, C_a, expressed in dpm/ml. This resulted in the V_c term with the units, ml/g dry wt. V_c derived here is equivalent to the distribution volume of the compartmental models used to describe the metabolic kinetics for PET tracers. As a second approach, TR was normalized by the specific activity of the arterial blood and used to estimate the amount of fatty acids incorporated into or displaced from V_c over the course of the perfusion trials. The units for this expression are given as μmol/g dry wt. Specific activity was

calculated as the ratio of the arterial radioactivity of the tracer to the arterial concentration of free fatty acids (dpm/μmol).

Figure 3 is an example of the time course of equilibrium labeling of radioactive fatty acids (Fig. 3A) and $^{14}CO_2$ (Fig. 3B) contained in the venous effluent measured after the beginning of infusion of labeled palmitate. The integral of Equation 2 is graphically represented by the shaded area in the figure. The interpolation line between the data points is derived by using the cubic spline technique. The equilibration value, C_{ss}, is the horizontal line and is the average of the last 35 min (for free fatty acid) and the last 10 min (for CO_2) of venous sampling. The data depicted in this figure are the rates of radioactivity (in dpm) leaving the myocardium per minute through the venous efflux normalized by both the total radioactivity of the artery (in dpm) and the tissue weight of the LAD-perfused myocardium.

Washout of the radioactive isotope was also examined in seven animals. The trapped radioactive material which remained in the heart when the infusion of the tracer was terminated is the summation of the venous efflux given by:

$$TR = F_c \times \int_0^{\infty} C(t) \times dt \qquad \text{Eq. 3}$$

and

$$V_c = TR \div C_a. \qquad \text{Eq. 4}$$

The darkly shaded areas in Figure 4 are the corresponding carbon pools for FFA and $^{14}CO_2$ from one animal. Washout of radioactive palmitate is shown in Figure 4A. As with the uptake curves, the free fatty acid radioactive pool size was quite small and returned rapidly to zero. There was no evidence for release of labeled nonmetabolized fatty acids from stored tissue pools. Figure 4B depicts the much larger radioactive carbon pool that leaves the heart in the form of $^{14}CO_2$. With washout, the efflux of $^{14}CO_2$ dropped to an intermediate level and remained there for the duration of the sampling period. This lower level (hatched bars) represents release of product from a storage tissue pool with a very long time constant. The efflux of $^{14}CO_2$ never reached zero in these experiments, and the decay rate of this pool was too slow to allow for an accurate determination of the long time constants or their distribution volumes in all cases. Instead, the level of the CO_2 radioactivity at the last sample time was tabulated and a ratio constructed with reference to the equilibration level obtained from the uptake curves. Since the $^{14}CO_2$ efflux in the washout experiments never reached zero, non equilibrium of labeling is suggested. The ratio of CO_2 washout to uptake, listed below, served as a measure of this non equilibration.

Direct Observations

For technical reasons involving early problems in establishing the input function of radioactivity (establishing the proper mixing and infusion speeds), identical measurements were not made in all animals. The mean values of individual parameters are listed in Tables 1–4. The hemodynamic and metabolic status and availability of substrates in the perfusate for all animals are represented in Table 1. Left ventricular pressure was controlled by the regulation of blood volume with 6% dextran. The respirator was adjusted and sodium bicarbonate used to maintain blood gases at normal values. Substrate levels were those of whole blood and blood glucose was supplemented periodically to maintain physiological levels. There were essentially no changes in these variables from the beginning to the end of the studies or among animals as reflected by the small s.e.m. values. The only variable which did vary among animals (but not as a function of perfusion time for any one animal) was heart rate which ranged from 106 to 217 bpm (mean 153 ± 8 bpm). Levels of oxygen consumption were compatible with aerobic values previously reported in this heart model (*12,13*) and were essentially unchanged over time.

In separate experiments, blood samples from five animals were taken 40 min after infusion of palmitate and

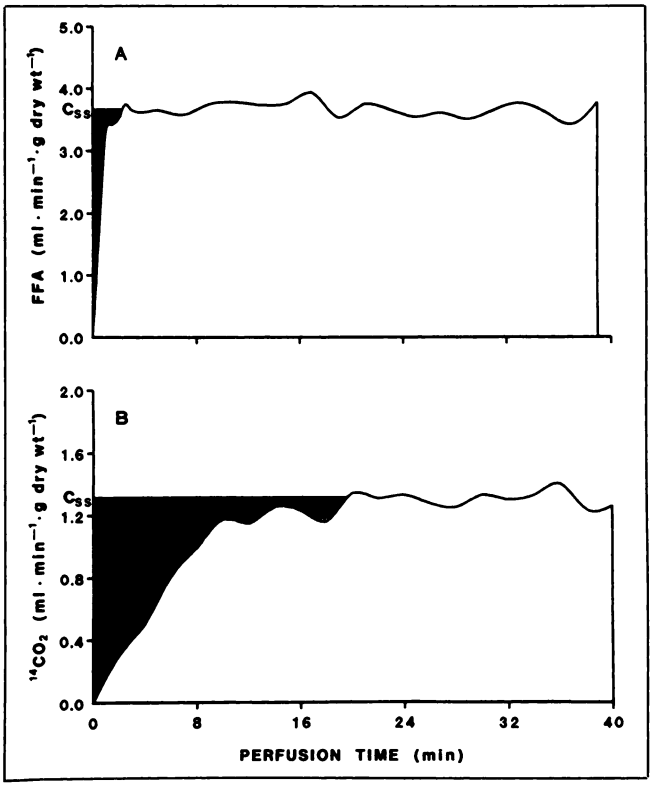

FIGURE 3. Experimental data from one animal showing actual curves of step-function, equilibrium labeling of [^{14}C]palmitate as monitored from efflux of counts (ml min^{-1} g dry wt^{-1}) in coronary venous blood for fatty acids (A) and $^{14}CO_2$ (B). The shaded area extrapolated back from steady state levels of either metabolite represents the carbon pool size within the myocardial utilization pathway. C_{ss} represents the steady-state concentration of radioactive end-metabolite in venous blood. The fatty acid pool is small and is most likely contained within the perfusate blood volume.

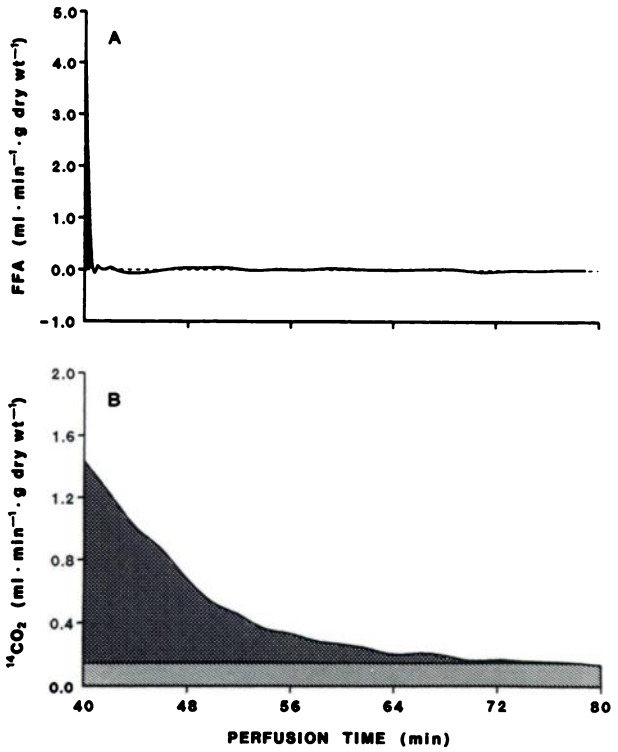

FIGURE 4. Experimental data from one animal showing actual curves of step-function termination of equilibrium labeling of ^{14}C-palmitate as monitored from efflux of counts (ml min^{-1} g dry wt^{-1}) in coronary venous blood for fatty acids (A) and $^{14}CO_2$ (B). Again, the fatty acid pool is quite small and quickly reaches zero volume. Conversely, the decay of counts for CO_2 is larger and never reaches zero value, suggesting the interaction of another tissue carbon pool with a very long time constant (hatched bars).

were analyzed for distribution of radioactivity among metabolites from venous effluent as indicated in Figure 2. This time period had the maximum potential for detecting any radioactivity which was contained in metabolites released into efflux. The results of this analysis are shown in Table 2. Each fraction is expressed as a percent of the total radioactivity. To estimate the amount of background radioactivity from ^{14}C-palmitate in perfusate, analysis was also performed on unlabeled pig blood to which 60,000 dpm/ml ^{14}C-palmitate (approximately that infused during the in vivo studies) was added. These counts, also shown in Table 2, served as a standard to which the in vivo samples were compared. There were no counts in the in vivo blood samples above that which were found in the standards except for the cholesterol fraction which was only slightly increased. Background $^{14}CO_2$ levels in standard blood were almost zero (50 of 60,000 dpm/ml). Virtually all of the radioactivity in the venous efflux from the in vivo studies was in the form of either $^{14}CO_2$ (not shown in Table 2) or ^{14}C-palmitate. Background radioactivity exclusive of CO_2 and fatty acids were insufficient to identify any other metabolites by HPLC techniques.

Distribution volumes for these two constituents as calculated by Equations 2 and 4 are included in Table 3. The integrals of the uptake and washout curves were normalized and expressed both as ml/g dry wt and μmol/g dry wt. There were no statistical differences between the uptake and washout estimates for $^{14}CO_2$ pool size. The fatty acid distribution volume was slightly larger in magnitude from uptake as compared with washout curve analysis ($p < 0.03$–0.045). A fatty acid pool was also derived for the intravascular space between the arterial injection site and the venous sampling site. This volume includes a vascular volume calculated as 11% of the tissue bed weight perfused by the LAD circuit and 8 ml of catheter volume. The 11% coronary blood volume had been previously obtained in

TABLE 1
Hemodynamic, Perfusate, and Metabolic Parameters in the Animal Population

Variables	Perfusion time* 0 min	Perfusion time* 40 min
LVP (mmHg)	102 ± 2	102 ± 2
LVEDP (mmHg)	6.6 ± 0.7	5.3 ± 0.6
Arterial pH	7.42 ± 0.02	7.42 ± 0.02
Arterial O_2 sat (%)	98.1 ± 0.8	97.6 ± 0.9
Arterial glucose (μmol/ml)	7.4 ± 1.4	7.1 ± 1.1
Arterial FFA (μmol/ml)	0.48 ± 0.05	0.44 ± 0.04
HR (bpm)	153 ± 8	156 ± 8
MVO_2 (mmol hr^{-1} g dry wt^{-1})	1.46 ± 0.11	1.49 ± 0.09

* No statistical differences were calculated in any of the variables between 0 and 40 min perfusion.

LVP = left ventricular systolic pressure; LVEDP = left ventricular end-diastolic pressure; (n = 20) O_2 sat = oxygen saturation; FFA = free fatty acid; HR = heart rate; MVO_2 = myocardial oxygen consumption.

TABLE 2
Distribution of Radioactivity in Blood in Five Animals

Phase fractions	Venous %	Standard* %	p^{11}
Aqueous	10.37 ± 0.90	5.70 ± 2.55	ns
Organic	89.25 ± 0.91	93.90 ± 2.52	ns
Total of two phases	99.62 ± 0.04	99.60 ± 0.04	ns
Total direct (plasma)	100	100	—
Lipid Species			
Cholesteryl Ester	0.12 ± 0.03	0.08 ± 0.02	ns
Triglycerides	0.08 ± 0.01	0.10 ± 0.05	ns
FFA	81.06 ± 1.61	83.48 ± 2.58	ns
Cholesterol	0.86 ± 0.07	0.54 ± 0.04	<0.008
Phospholipids	0.67 ± 0.09	0.68 ± 0.23	ns
Total in Fractions	82.79 ± 1.59	84.88 ± 2.64	ns
Residue	6.52 ± 0.73	9.03 ± 2.20	ns
Total of all lipid species	89.30 ± 0.90	93.92 ± 2.50	ns
p^1	ns	ns	

* Standard is nonradioactive blood spiked with ^{14}C-palmitate (60,000 dpm/ml).

p^1 describes the statistical comparisons of data between total of all lipid species and the organic phase fraction.

p^{11} describes the statistical comparisons between radioactivity in the coronary venous effluent and the "spiked" standards.

TABLE 3
Carbon Pool Sizes for CO_2 and Free Fatty Acids as Estimated by Uptake and Washout Function of Labeled Infusions of Palmitate

	Carbon Pool Size					
	CO_2		Free fatty acid		Free fatty acid	
Methods of analysis	ml/g dry	μmol/g dry	ml/g dry	μmol/g dry	ml/g dry	μmol/g dry
Uptake (n = 20)	15.8 ± 2.4	4.2 ± 0.8				
Washout (n = 7)	11.4 ± 2.2	3.6 ± 0.8				
P	ns	ns				
Uptake (n = 9)			1.7 ± 0.1	0.50 ± 0.07		
Washout (n = 7)			1.2 ± 0.2	0.41 ± 0.08		
P			$p < 0.045$	$p < 0.03$		
Volume* (n = 9)					1.4 ± 0.1	0.40 ± 0.06
P′					ns	ns
P″					$p < 0.036$	ns

* Volume method was calculated as 8 ml (volume in perfusate tubing) + 11% (coronary blood volume contained i myocardial tissue weight) × tissue weight. All data were normalized by tissue dry wt.

P compares results estimated by uptake and washout methods; P′ by washout and volume methods; and P″ by uptake and volume methods.

this laboratory using ^{14}C-dextran as a plasma marker (*21*). These calculations were comparable to those estimated by Equations 2 and 4 (except for a slightly lower value statistically from that of the uptake method in ml/g dry wt) and suggested that for all practical purposes the in vivo fatty acid distribution volume could be attributed to the radioactivity trapped in the perfusate.

The ratio of residual $^{14}CO_2$ production calculated from the washout and uptake curves and which served as an index of non equilibrium in step function labeling ranged from 0% to 11% (4.3% ± 1.5%) and reflected a large variability among animals. This ratio was influenced by changes in mechanical function as suggested by its correlation with heart rate ($^{14}CO_2$ ratio = $-17.6 + 0.2 \times$ heart rate; $r = 0.8$, $p < 0.03$). Thus, in the presence of tachycardia, nonequilibrium of steady-state labeling of fatty acid and lipid pools was enhanced.

The distribution of radioactivity among tissue products is given in Table 4. The tissue was extracted into an aqueous soluble and lipid phase. The sum of these two

TABLE 4
Distribution of Myocardial Tissue Counts of Radioactivity in the Animal Populations as Expressed in Fatty Acid Equivalents

	(μmol/g dry)			(ml/g dry)		
	Uptake (n = 11–12)	Washout (n = 7)	P	Uptake (n = 11–12)	Washout (n = 7)	P
Phase Fractions						
Aqueous soluble	3.6 ± 0.7	1.3 ± 0.2	<0.01	16.6 ± 1.9	3.9 ± 0.5	<0.05
Lipid	5.9 ± 1.3	7.7 ± 2.9	ns	24.6 ± 4.4	22.0 ± 5.8	ns
Total of two phases*	9.8 ± 1.6	8.9 ± 2.9	ns	41.8 ± 4.0	25.8 ± 5.5	<0.03
Total Direct	9.8 ± 1.8	8.6 ± 3.8	ns	41.6 ± 4.9	30.3 ± 7.0	ns
P′	ns	ns		ns	<0.05	
Lipid Species						
Triglycerides	3.7 ± 1.0	5.8 ± 2.7	ns	16.4 ± 3.9	15.9 ± 5.6	ns
Phospholipids	1.5 ± 0.2	1.5 ± 0.2	ns	4.0 ± 0.3	4.9 ± 0.7	ns
Cholesterol	0.3 ± 0.1	0.2 ± 0.1	ns	1.3 ± 0.3	0.7 ± 0.2	<0.06
Cholesteryl Esters	0.04 ± 0.01	0.04 ± 0.01	ns	0.15 ± 0.62	0.10 ± 0.10	<0.07
Tissue FFA	0.3 ± 0.1	0.08 ± 0.02	<0.06	1.1 ± 0.3	0.3 ± 0.1	<0.03
Total of all species	5.9 ± 1.5	7.7 ± 2.9	ns	24.8 ± 4.4	22.0 ± 5.8	ns
P″	ns	ns		ns	ns	

* Total values represent the means of the sums of the constituents for the phase fractions or lipid species.

P describes the comparison of data between uptake and washout animals; P′, the comparison between total counts measured separately and added in both phase fractions and total counts measured directly; and P″, the comparison between lipid counts measured separately in various component lipid species and added together and those of the lipid fraction measured directly. Data are normalized by tissue dry wt.

extracts was compared to the total counts measured directly in another sample of solubilized tissue. The lipid fraction was further subdivided into separate species of component lipids and fatty acids, and the total of these counts was compared to those measured directly in the lipid fraction. Finally, comparisons were also made contrasting the effects of uptake and washout on distribution of radioactivity. Tissue label at the end of uptake experiments was approximately equally divided between the aqueous soluble and lipid fractions (40% and 60%, respectively). The counts measured directly in the solubilized tissue were virtually identical to the sum of counts measured in the two fractions. Radioactivity in the lipid fraction was completely contained in triacylglycerols, phospholipids, cholesterol, cholesteryl esters and free fatty acids. The majority of counts was present in complex lipids (about 66% in triacylglycerols and another 25% in phospholipids). Total triacylglycerol stores were 19.9 ± 4.7 μmol/g dry wt of which 3.7 – 5.8 μmol/g dry wt (see Table 4) contained radioactivity. The effect of washout was most evident in the decreases in counts contained in the aqueous soluble phase and tissue free fatty acids, which together accounted for 76% of the lost radioactivity. Smaller decreases in radioactivity incurred during washout were also noted from cholesterol and cholesteryl esters.

Various data in Tables 3 and 4 were also compared by other means. As noted, the size of the estimated free fatty acid and $^{14}CO_2$ uptake pools was quite variable from one animal to the other. Nevertheless, a strong correlation was observed between the $^{14}CO_2$ uptake pool size and the combined radioactivities in the aqueous soluble and free fatty acid fractions in tissue (Fig. 5). Radioactivity in the latter pools was lost rapidly in the washout experiments and presumably did so through the conversion to $^{14}CO_2$. A linear correlation between the $^{14}CO_2$ distribution volume

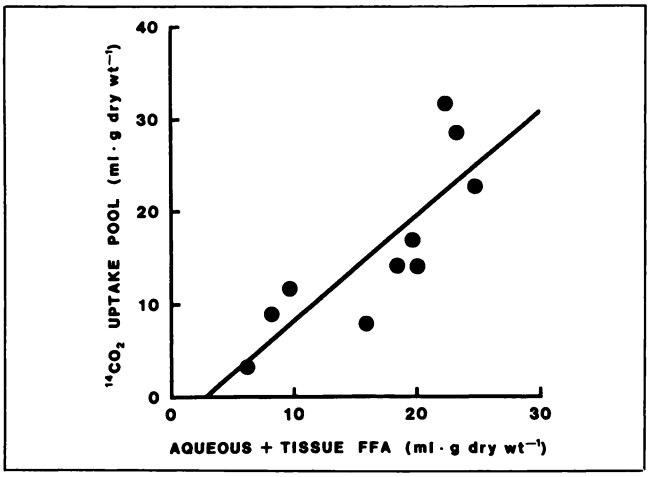

FIGURE 5. Linear correlation of $^{14}CO_2$ pool size estimated from input uptake curve analysis (displayed on the ordinate in ml/g dry wt) and actual counts contained in tissue represented by the aqueous soluble fraction and tissue fatty acids (displayed along the abscissa in ml/g dry wt). These two tissue compartments accounted for most of the $^{14}CO_2$ uptake pool ($r = 0.83$, $p < 0.004$, $n = 10$).

and the total radioactivity in the aqueous soluble fraction and tissue free fatty acids was expressed as:

$$V_{cCO_2} = -3.1 + 1.1 \times (\text{aqueous soluble fraction} + \text{tissue free fatty acid radioactivity}),$$

where $r = 0.83$ and $p < 0.004$ at $n = 10$.

It is likely that the pool identified by the $^{14}CO_2$ uptake curve, which includes only the pathway with the fast time constant, and the tissue radioactivity found in the aqueous soluble and free fatty acid fractions represent the same volume in tissue.

While the distribution volume of radioactivity in tissue phospholipids was relatively constant from animal to animal (2.6–5.3 ml/g dry wt), the radioactivity found in triacylglycerols in uptake infusion experiments was also quite variable (5.2–51.6 ml/g dry wt). The triacylglycerol radioactivity was negatively related to the radioactivity found in the aqueous soluble fraction as expressed by the relationship:

$$\text{Triacylglycerol radioactivity} = 45 - 1.74 \times \text{aqueous soluble fraction radioactivity},$$

where $r = 0.76$ and $p < 0.01$ at $n = 10$.

The aqueous soluble and triacylglycerol fractions in tissue in turn may be related to the metabolic demands of the heart as reflected by oxygen consumption values and to the production of $^{14}CO_2$ at the conclusion of the uptake infusion experiments (Fig. 6). Basically, the aqueous soluble fraction and tissue free fatty acid fraction (Fig. 6A) were large if the production of radioactive CO_2 from exogenous substrate was high. This tended to occur at low or intermediate levels of myocardial oxygen consumption (MVO_2). The relationship was expressed as:

$$\text{Aqueous soluble fraction + tissue FFA radioactivity} = 23.9 - 11.8 \times MVO_2 + 7.7 \times {}^{14}CO_2,$$

where $r = 0.92$ and $p < 0.002$ at $n = 10$. The probabilities that the individual regression coefficients were zero were $p < 0.002$ for MVO_2 and $p < 0.004$ for $^{14}CO_2$, respectively.

Conversely, tissue triacylglycerols (Fig. 6B) were high when $^{14}CO_2$ production was low tended to occur at intermediate-to-high levels of myocardial oxygen consumption. The relationship was expressed as:

$$\text{Triacylglycerol radioactivity} = 17.4 + 16.5 \times MVO_2 - 18.1 \times {}^{14}CO_2,$$

where $r = 0.77$ and $p < 0.001$ at $n = 18$. Here the probabilities that the individual regression coefficients were zero were $p < 0.024$ for MVO_2 and $p < 0.001$ for $^{14}CO_2$, respectively.

We interpret these correlations in the following way. In hearts where oxygen consumption and $^{14}CO_2$ production

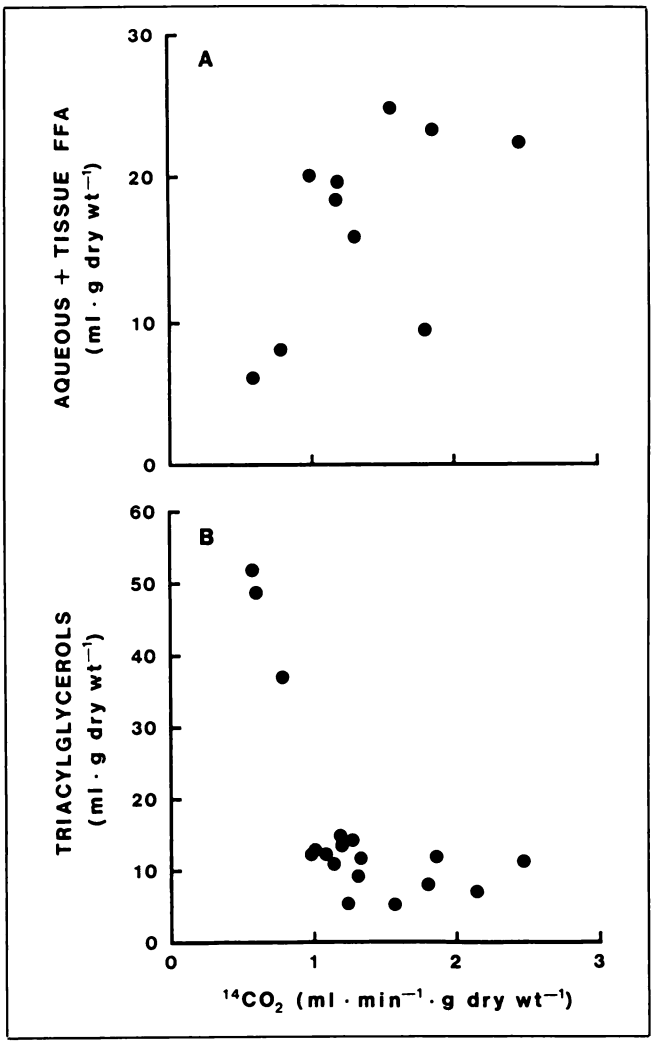

FIGURE 6. Linear correlations of tissue distribution of counts (panel A includes data for the aqueous soluble fraction and tissue fatty acids displayed on the ordinate in ml/g dry wt; panel B includes tissue triacylglycerols on the ordinate in ml/g dry wt) arrayed with the metabolic state of the myocardium as represented by the steady state production of $^{14}CO_2$. The correlation of panel A is positive ($r = 0.92$, $p < 0002$, $n = 10$), while panel B is negative ($r = -0.77$, $p < 0.001$, $n = 18$).

from exogenous palmitate are in close approximation, the above relationships suggest that the majority of radioactivity is contained in the aqueous soluble fraction which proceeds rapidly to fatty acid oxidation. In this instance, equilibrium labeling with exogenous substrate accurately represents the behavior of endogenous fatty acids. Conversely, if the levels of oxygen consumption and $^{14}CO_2$ production from exogenous palmitate are disparate, suggesting delays in equilibrium labeling, the majority of counts are trapped and only slowly released from the triacylglycerol pool. This lipid storage pool with a very slow constant prevents rapid labeling of the fatty acid pathway. In this instance, equilibrium labeling with exogenous substrate does not well describe the metabolic storage and release of endogenous fatty acids. This must be remembered when interpreting rates of substrate utilization data and may influence the results of such descriptions.

DISCUSSION

The purpose of the present report was to examine the rate of appearance and disappearance of radioactive metabolites from venous effluent in aerobically perfused hearts after either a step-function increase or decrease in radioactivity supplied by labeled palmitate. We have previously used this tracer to estimate rates of fatty acid oxidation by steady state production of $^{14}CO_2$ (*1,9–11,22, 23*) but have never previously evaluated the transients by this labeling technique. Characterization of these transients is of interest in light of recent data, which suggested that the fatty acid utilization pathway passes through a previously recognized (*4*) but under-appreciated, functionally large, triacylglycerol storage pool on its way to CO_2 production (*5*). Residence time of exogenously labeled fatty acid within this pool was unexpectedly long and presents difficulties for external labeling techniques. In such conditions, the calculated rate of metabolic oxidation may be an underestimate of the true metabolic rate for endogenous fatty acids. Describing the magnitude and kinetic properties of this pool is practically useful also to better understand the information currently being derived from ^{11}C-palmitate in studies using positron emission tomography. This latter approach, which has been employed to estimate fatty acid utilization in both humans and experimental animals (*24–27*), relies on measuring the washout of a short-lived, radioactive tracer from various storage pools. As suggested by the present data, use of this isotope may be confounded by the long release times of neutral lipids and result in incomplete characterizations of the more distal elements in the fatty acid utilization pathway. Such an influence must be accounted for in the modeling of kinetic data so that accurate interpretations are possible using this modality.

The animal model system used in our laboratory has been extensively described elsewhere (*1,9–12,14,22,23*). A few further comments are provided. The experiments were performed in working, *in situ* hearts perfused with arterial blood via a perfusion circuit which included modest levels (3.6%) of labeled products returning from the periphery. This recirculation prohibited the use of an inert vascular indicator which, unlike ^{14}C-palmitate, would not be removed by the periphery. Without such a tracer, it is impossible to preclude the existence of a small nonvascular component in the calculated free fatty acid distribution volumes. However, to the best of our knowledge, given the large range of intravascular values previously published for this space, i.e., 4.8–14.4 ml/100 g wet wt (*27*), it seems reasonable to conclude that all of the labeled free fatty acid in venous effuent resided in the vascular volume. The reason why the pool size of free fatty acid appeared smaller in the washout as compared with the uptake curves, unlike those for the $^{14}CO_2$ curves, is unclear but probably reflected

the deadspace in the tracer infusion system which would have influenced the uptake curves.

Only approximately half of the radioactivity in tissue was accounted for by the calculated pool sizes of free fatty acids and CO_2 from venous monitoring, and virtually all of this was contained in the $^{14}CO_2$ pool. The remainder of the tissue radioactivity was assumed to be hidden in a pool, presumably triacylglycerols, with very slow turnover which was only revealed by the CO_2 washout experiments. These studies also defined the more volatile tissue spaces, particularly those identified by the aqueous soluble and free fatty acid radioactivities and to a lesser extent the cholesterol and cholesteryl ester lipid pools. With washout, the radioactivity remaining in the heart was in the triacylglycerol and phospholipid fractions. The tissue pool size delineated by efflux of $^{14}CO_2$ was similar to and correlated well with the combined radioactivities in the tissue aqueous soluble and free fatty acid fractions and probably represented the same pool.

The other main finding, particularly evident from the washout experiments, was that all the pools (lipids and aqueous soluble) had one common pathway which resulted in the efflux of radioactivity as $^{14}CO_2$. There was no other significant radioactivity released from the heart. The washout data demonstrated a large storage pool within the fatty acid utilization pathway which cannot be ignored kinetically in its contribution to fatty acid oxidation. This pool has long been recognized in biochemical analysis (*4*), but its functional importance and confounding influence to exogenous substrate labeling protocols have been underappreciated. Our results have implications both for studies in which the steady state production of $^{14}CO_2$ is used as a measure of fatty acid oxidation and in those using positron emission tomography in which the isotope cannot easily interrogate pools with slow turnover and release characteristics without appropriate modeling schemes. We calculate that the storage pool of triacylglycerols from uptake radioactivity experiments accumulates about 4 μmol/g dry wt of free fatty acid. The heart has approximately 20 μmol free fatty acid/g dry wt contained in triacylglycerols, and labeled entry into this pool displaces fatty acids which are almost entirely unlabeled. These 4 μmol of unlabeled free fatty acid/g dry wt, when readmitted back into the utilization pathway, amounts to approximately 0.1 μmol min^{-1} g $dry\ wt^{-1}$ which, when added to the 0.4 μmol min^{-1} g $dry\ wt^{-1}$ free fatty acid measured from steady-state of production of $^{14}CO_2$, yields a sum of about 0.5 μmol min^{-1} g $dry\ wt^{-1}$. Thus, 20% of fatty acid oxidation on the average is from unlabeled substrate and as such goes unmeasured. Many of the hearts in these studies had an even larger pool of radioactivity trapped as neutral lipids.

The relationship between the radioactivity in the major tissue compartments and the metabolic state of the heart (Fig. 6B) can be explained by hypothesizing two parallel routes for the fatty acid utilization pathway which converge to a final common pathway. In one track of the model, the radioactive palmitate enters the cell, is activated and directly enters mitochondria (assumed to be in the aqueous soluble fraction) where it is oxidized, and the radioactive tracer released as $^{14}CO_2$. In the other route, the labeled fatty acid enters the cell, is activated, but then is taken up into the triacylglycerol pool. The pool is eventually hydrolyzed but most likely in the early time periods, unlabeled fatty acids are released to proceed to oxidation. As previously recognized, the triacylglycerol pool is quite large (*4,5*), and its labeling by ^{14}C-palmitate remains dilute such that the ^{14}C-palmitate molecules effectively become trapped. By this hypothesis, two extremes are possible. In one case, all the ^{14}C-palmitate may enter the triacylglycerol pool and stay trapped with no subsequent production of $^{14}CO_2$. No radioactivity is measured in the aqueous fraction, and a large collection of counts accumulates in the triacylglycerol pool. In the other extreme, the triacylglycerol pool is bypassed completely, and fatty acids are directly oxidized. Production of $^{14}CO_2$ is high and the aqueous fraction contains a large amount of radioactivity while the triacylglycerol pool is virtually depleted of label. The present data represent an intermediate position between these two extremes.

The main purpose of this report was to describe the metabolic performance of aerobically perfused myocardium and to define the rates of oxidation of its principal substrate, long-chain fatty acids, using external labeling techniques. As such and assuming equilibrium labeling during the time course of our perfusion trials, there should have been close approximation between oxygen consumption and fatty acid oxidation estimated by steady state production of $^{14}CO_2$ from exogenous palmitate. However, the labeled palmitate trapped in complex lipids prevented complete equilibrium labeling and created a discrepancy between oxygen consumption and the estimates of fatty acid oxidation. The more radioactivity trapped, the larger the discrepancy, thus explaining the negative correlation between the tissue triacylglycerol pool size with $^{14}CO_2$ production and the positive correlation with MVO_2 (Fig. 6B). On the other hand, as less radioactivity was trapped, the discrepancy between oxygen consumption and $^{14}CO_2$ decreased as more radioactivity was diverted directly into and through the aqueous soluble fraction. Consequently, there was a positive correlation between the aqueous soluble pool size and $^{14}CO_2$ production and a negative correlation with MVO_2 (Fig. 6A). This discrepancy, which is a function of the relative flux rates in each of the two arms of the fatty acid utilization pathway leading to fatty acid oxidation, imparts an error in estimating rates of substrate oxidation in the myocardium. This error is highly variable and may be substantial in some animals.

ACKNOWLEDGMENTS

The authors thank T.M. Lange, S.K. Rasmussen, D.K. Paulson, E. Scarborough and C.R Kidd for technical assistance.

This work was supported in part by PHS grant HL-41914, the

Rennebohm Foundation of Wisconsin and the Oscar Mayer Cardiovascular Research Fund.

REFERENCES

1. Liedtke AJ, DeMaison L, Eggleston AM, Cohen LM, Nellis SH. Changes in substrate metabolism and effects of excess fatty acids in reperfused myocardium. *Circ Res* 1988;62:535–542.
2. Oram JF, Bennetch SL, Neely JR. Regulation of fatty acid utilization in isolated perfused rat hearts. *J Biol Chem* 1973;248:5299–5309.
3. Wisneski JA, Gertz EW, Neese RA, Mayr M. Myocardial metabolism of free fatty acids: Studies ^{14}C-labeled substrates in humans. *J Clin Invest* 1987;79:359–366.
4. Neely JR, Morgan HE. Relationship between carbohydrate and lipid metabolism and the energy balance of heart muscle. *Ann Rev Physiol* 1976;36:413–459.
5. Hansen CA, Fellenius E, Neely JR. Metabolic rates in normal and infarcted myocardium. *Can J Cardiol, July Suppl* 1986;(suppl A):1A–8A.
6. Lerch RA, Bergmann SR Ambos HD, Welch MJ, Ter-Pogossian MM, Sobel BE. Effect of flow-independent reduction of metabolism on regional myocardial clearance of ^{11}C-palmitate. *Circulation* 1982;65:731–738.
7. Schelbert HR, Henze E, Keen R, et al. C-11 palmitate for the noninvasive evaluation of regional myocardial fatty acid metabolism with positron-computed tomography. IV. In vivo evaluation of acute demand-induced ischemia in dogs. *Am Heart J* 1983;106:736–750.
8. Nellis SH, Liedtke AJ, Renstrom B. Distribution of carbon flux within fatty acid utilization during myocardial ischemia and reperfusion. *Circ Res* 1991;69:779–790.
9. Miller WP, Liedtke AJ, Nellis SH. Effects of 2-tetradecylglycidic acid on myocardial function in swine hearts. *Am J Physiol* 1986;251(*Heart Circ Physiol* 20):H547–H543.
10. Molaparast-Saless F, Liedtke AJ, Nellis SH. Effects of the fatty acid blocking agents, oxfenicine and 4-bromocrotonic acid, on performance in aerobic and ischemic myocardium. *J Mol Cell Cardiol* 1987;19:509–520.
11. Liedtke AJ, Demaison L, Nellis SH. Effect of L-propionylcarnitine on mechanical recovery from ischemia/reflow in intact hearts. *Am J Physiol* 1988;255(*Heart Circ Physiol* 24):H169–H176.
12. Renstrom B, Nellis SH, Liedtke AJ. Metabolic oxidation of glucose during early myocardial reperfusion. *Circ Res* 1989;65:1094–1101.
13. Renstrom B, Nellis SH, Liedtke AJ. Metabolic oxidation of pyruvate and lactate during early myocardial reperfusion. *Circ Res* 1990;66:282–288.
14. Liedtke AJ, Nellis SH, Neely JR. Effects of excess free fatty acids on mechanical and metabolic function in normal and ischemic myocardium in swine. *Circ Res* 1978;43:652–661.
15. Pokits B, Paschke A, Roscher A. Simultaneous quantitation of lactic and pyruvic acid in blood by high performance liquid chromatography. *J Clin Chem* 1986;24:811–812.
16. Ho RJ. Radiochemical assay of long-chain fatty acids using ^{63}Ni as tracer. *Anal Biochem* 1970;36:105–113.
17. Bligh EG, Dyer WJ. A rapid method of total lipid extraction and purification. *Can J Biochem Physiol* 1959;37:911–917.
18. Hamilton JG, Comai K. Rapid separation of neural lipids, free fatty acids and polar lipids using prepacked silica Sep-Pak columns. *Lipids* 1988;23:1146–1149.
19. Liedtke AJ, Nellis SH. Effects of buffered pyruvate on regional cardiac function in moderate, short-term ischemia. *Circ Res* 1978;43:189–199.
20. Bier J, Sharaf B, Gewertz H. Origin of anterior interventricular vein blood in domestic swine. *Am J Physiol* 1991;260(*Heart Circ Physiol* 29):H1732–H1736.
21. Miller WP, Nellis SH, Liedtke AJ, Whitesell L, Effron BA. Coronary hyperfusion and ventricular function in intact and isovolumic pig hearts. *Am J Physiol* 1990;258(*Heart Circ Physiol* 27:H500–H507.
22. Liedtke AJ, Nellis SH. Effects of carnitine isomers on fatty acid metabolism in ischemic hearts. *Circ Res* 1981;48:859–866.
23. Liedtke AJ, Nellis SH, Whitesell LF. Effects of regional ischemia on metabolic function in adjacent aerobic myocardium. *J Mol Cell Cardiol* 1982;14:195–206.
24. Grover-McKay M, Schelbert HR, Schwaiger M, et al. Identification of impaired metabolic reserve by atrial pacing in patients with significant coronary artery stenosis. *Circulation* 1986;74:281–292.
25. Schwaiger M, Schelbert HR, Ellison D, et al. Sustained regional abnormalities in cardiac metabolism after transient ischemia in the chronic dog model. *J Am Coll Cardiol* 1985;6:336–347
26. Schwaiger M, Schelbert HR, Keen R, et al. Retention and clearance of C-11 palmitic acid in ischemic and reperfused canine myocardium. *J Am Coll Cardiol* 1985;6:311–320.
27. Spaan JAE. Coronary diastolic pressure-flow relation and zero pressure explained on the basis of intramyocardial compliance. *Circ Res* 1985;56:293–309.